Regimes of suprathermal electron transport

Michael E. Glinsky
Lawrence Livermore National Laboratory, Livermore, California 94550

(Received 7 October 1994; accepted 27 March 1995)

Regimes of the one-dimensional (1-D) transport of suprathermal electrons into a cold background plasma are delineated. A well ordered temporal progression is found through eras where $J \cdot E$ heating, hot electron–cold electron collisional heating, and diffusive heat flow dominate the cold electron energy equation. Scaling relations for how important quantities such as the width and temperature of the heated layer of cold electrons evolve with time are presented. These scaling relations are extracted from a simple 1-D model of the transport which can be written in dimensionless form with one free parameter. The parameter is shown to be the suprathermal electron velocity divided by the drift velocity of cold electrons which balances the suprathermal current. Special attention is paid to the assumptions which allow the reduction from the collisional Vlasov equation, using a Fokker–Planck collision operator, to this simple model. These model equations are numerically solved and compared to both the scaling relations and a more complete multigroup electron diffusion transport. Implications of the scaling relations on fast ion generation, magnetic field generation, and electric field inhibition of electron transport are examined as they apply to laser heated plasmas. © *1995 American Institute of Physics.*

I. INTRODUCTION

The interaction of a laser beam with a plasma can produce energetic electrons that are well above the background electron thermal temperature. These suprathermal or hot electrons can be generated by various mechanisms which include resonant absorption,[1] $J \times B$ heating,[2,3] stimulated Raman scattering,[4] and not-so-resonant absorption.[5] Once the suprathermal electrons are made, they transport into the overdense background plasma. This transport is nonlocal due to the large mean free path of the hot electrons. In the past, this has been the subject of much research[6–14] because the performance of inertial confinement fusion target designs is dependent on this transport.[15,16] Models such as double diffusion,[6] multigroup diffusion,[17] and a Fokker–Planck expansion[11–13] have been developed and solved numerically. These models describe the plasma evolution with increasing degrees of sophistication as one goes forward in the list. What this paper adds to this research is not a more complete model, but a more global understanding of the interplay between the physical processes which determine the character of the suprathermal transport. These are $J \cdot E$ heating (slowing down the hot electrons by an electric field set up to draw a return current in the resistive cold background), drag heating (slowing down the hot electrons by direct collisions between the hot and cold electrons), and thermal heat conduction.

The results of this research can be applied to situations where a population of suprathermal electrons penetrates into a collisional plasma. Another example of such a situation is the propagation of intense electron beams through the atmosphere.[18]

We start by deriving, in Sec. II, a simple set of two coupled partial differential equations which describe the one-dimensional (1-D) penetration of a constant flux of hot electrons into a cold background plasma of large constant density. Special attention is paid to the approximations that are required to derive them. The result is a well-justified model that is essentially the same as the phenomenological double-diffusion model in many respects.

Section III defines the structure on which we examine the transport. First, the transport equations are put in dimensionless form. It is found that the solution of these equations depends on only one free dimensionless parameter (assuming constant atomic number, Z). This parameter is shown to be the hot electron velocity divided by the drift velocity of cold electrons which balances the suprathermal current. We continue in the analysis of the transport equations and find that there are five regimes of transport which always occur in the same temporal order. How important quantities such as the width and temperature of the heated layer scale with time are also found for each of these regimes.

The validity of an important assumption in the derivation of the transport model is examined in Sec. IV. This assumption, that there is only one group of hot electrons, is compared with the multigroup diffusion of hot electrons employed in the computer code LASNEX.[19] No significant differences are found.

Implications and applications of our model are looked at in Sec. V. These include fast ion generation, electric field inhibition of transport, magnetic field generation, and delineation of vastly different plasma and laser parameters (by orders of magnitude) which have similar transport.

We wish to caution the reader that we have only examined collisional transport. Other effects such as instabilities (e.g., two-stream[20,21] and ion acoustic[22]), and two-dimensional (2-D) phenomena (e.g., spatial spreading of the current, and large self-generated magnetic fields[23,24]) may influence the transport. One must examine the particular situation to see whether one of these complications should be included as an anomalous resistivity or another modification to the transport.

 1070-664X/95/2(7)/2796/11/$6.00

II. DERIVATION OF THE TWO GROUP MODEL

We proceed by deriving a "two group" electron model from the Vlasov equation with a Fokker–Planck collision operator,

$$\frac{\partial f_\alpha}{\partial t}+\mathbf{v}\cdot\frac{\partial f_\alpha}{\partial \mathbf{x}}+\frac{Z_\alpha e}{m_\alpha}\mathbf{E}\cdot\frac{\partial f_\alpha}{\partial \mathbf{v}}=\sum_\beta C(f_\alpha,f_\beta), \tag{1}$$

where the subscripts α and β will refer to the three particle species: ions, hot electrons, and cold electrons (i.e., i, h, and c, respectively). Magnetic fields have been neglected because a 1-D symmetry will be assumed. The standard form of the Coulomb collision operator[25] is used:

$$C(f_\alpha,f_\beta)=-\frac{\partial}{\partial \mathbf{v}}\cdot\mathbf{S}_{\alpha\beta}, \tag{2}$$

where

$$\mathbf{S}_{\alpha\beta}=\left\langle\frac{\Delta\mathbf{v}}{\Delta t}\right\rangle_\beta f_\alpha-\frac{1}{2}\frac{\partial}{\partial \mathbf{v}}\cdot\left\langle\frac{\Delta\mathbf{v}\Delta\mathbf{v}}{\Delta t}\right\rangle_\beta f_\alpha, \tag{3}$$

$$\left\langle\frac{\Delta\mathbf{v}}{\Delta t}\right\rangle_\beta=\frac{4\pi(Z_\alpha Z_\beta)^2e^4\ln\Lambda}{m_\alpha^2}\left(1+\frac{m_\alpha}{m_\beta}\right)\times\frac{\partial}{\partial \mathbf{v}}\int\frac{d^3\mathbf{v}'\,f_\beta(\mathbf{v}')}{|\mathbf{v}-\mathbf{v}'|}, \tag{4a}$$

and

$$\left\langle\frac{\Delta\mathbf{v}\Delta\mathbf{v}}{\Delta t}\right\rangle_\beta=\frac{4\pi(Z_\alpha Z_\beta)^2e^4\ln\Lambda}{m_\alpha^2}\times\frac{\partial}{\partial \mathbf{v}}\frac{\partial}{\partial \mathbf{v}}\int d^3\mathbf{v}'|\mathbf{v}-\mathbf{v}'|f_\beta(\mathbf{v}'). \tag{4b}$$

The distribution functions are normalized in the common way so that

$$\int f_\alpha(\mathbf{x},\mathbf{v},t)d^3\mathbf{v}=n_\alpha(\mathbf{x},t). \tag{5}$$

Simplified forms of the distribution functions are used:

$$f_i(\mathbf{x},\mathbf{v},t)=\frac{n_c}{Z}\,\delta(\mathbf{v}), \tag{6a}$$

$$f_c(\mathbf{x},\mathbf{v},t)=n_c\left(\frac{m_e}{2\pi T_c(\mathbf{x},t)}\right)^{3/2}\exp\left(-\frac{mv^2}{2T_c(\mathbf{x},t)}\right)+\hat{\mathbf{v}}\cdot\boldsymbol{\delta}f(\mathbf{x},v,t)=f_c^{(0)}+f_c^{(1)}, \tag{6b}$$

and

$$f_h(\mathbf{x},\mathbf{v},t)=n_h(\mathbf{x},t)\,\delta(v-\sqrt{3T_h/m})g(\Omega); \tag{6c}$$

where $g(\Omega)$ is distribution function in velocity solid angle for the hot electrons, and both the n_c and T_h are constants. There are several assumptions implicit in the assumed form of the distribution functions that need to be examined in more detail. The first is that n_c is a constant. This will be true provided that (1) the length scales of interest are much larger than a cold electron Debye length, $L\gg\lambda_{Dc}$, so that quasineutrality is maintained; (2) there is not sufficient time for the ions to move, $t<L/(ZT_h/m_i)^{1/2}$; and (3) the hot electron density is small compared to cold electron density, $n_h\ll n_c$. When combined together, the above three conditions imply

$$\text{constant}=\overset{(2)}{n_i}=\overset{(1)}{n_c}+\overset{(3)}{n_h}\approx n_c$$

as desired. The second assumption is that the cold electron distribution function velocity expansion can be truncated as shown. This will be true as long as the length and time scales of interest are greater than the cold electron–ion mean free path and mean collision time. The nonlocal transport of the hot electron component guarantees this, because the long mean free path and collision time of the hot electrons determines the relevant scales. But this leads us to the third assumption that there is only one group of hot electrons with a fixed temperature. What should be done is to have many groups of hot electrons which are coupled together as is done in multigroup diffusion.[17] For the sake of simplicity of the resulting model, we have retained only one group. This will make it simple to derive scaling relationships. It will have to verified *a posteriori* that adding more groups will not change the result. This will be done in Sec. IV.

Since we are going to be interested in scaling behavior of the solutions, the assumption is made that the plasma is Lorentzian,[26] or equivalently $Z\gg1$. This will modify the transport coefficients by factors of order 2 for the case of hydrogen, but will give the correct large Z scaling for the coefficients.

Parts of the following derivation may be found in some of the references.[7–9,26,27] What we wish to focus on are the assumptions made in obtaining the simple model and the way in which the two electron groups are coupled. The reader is referred to these external sources to fill in the gaps between some of the equations.

First, consider the equation for the cold electrons:

$$\frac{\partial f_c}{\partial t}+\mathbf{v}\cdot\frac{\partial f_c}{\partial \mathbf{r}}-\frac{e}{m_e}\mathbf{E}\cdot\frac{\partial f_c}{\partial \mathbf{v}}=C(f_c,f_i)+C(f_c,f_h), \tag{7}$$

where we have neglected the cold electron self-collision term since it will not contribute to the moment equations. This is because particle number, total momentum, and total energy are conserved in Coulomb collisions.[27] Assuming $m_e\ll m_i$, one can reduce the cold electron ion collision operator to the following form:

$$C(f_c,f_i)=-f_c^{(1)}/\tau_{ei}(v), \tag{8}$$

where

$$\tau_{ei}(v)\equiv\frac{m_e^2v^3}{4\pi Zn_ce^4\ln\Lambda}, \tag{9}$$

and $\ln\Lambda$ is the usual Coulomb logarithm. We now solve for $f_c^{(1)}$ by substituting $f_c^{(0)}$ for f_c in Eq. (7), and by using the form of $C(f_c,f_i)$ given in Eq. (8). The result is

$$f_c^{(1)}=-\tau_{ei}(v)\left(\frac{\partial f_c^{(0)}}{\partial t}+\mathbf{v}\cdot\frac{\partial f_c^{(0)}}{\partial \mathbf{x}}-\frac{e}{m_e}\mathbf{E}\cdot\frac{\partial f_c^{(0)}}{\partial \mathbf{v}}-C(f_c^{(0)},f_h)\right). \tag{10}$$

To obtain the momentum equation take the first velocity moment of Eq. (10). One is left with

$$\mathbf{E}=\frac{\mathbf{J}}{\sigma}-\frac{5}{2}\frac{1}{e}\nabla T_c-\frac{\mathbf{R}_h}{en_c}, \tag{11}$$

where

$$\mathbf{J}\equiv\int e\mathbf{v}f_c^{(1)}\,d^3\mathbf{v}, \tag{12}$$

$$\sigma\equiv\frac{4\sqrt{2}}{\pi^{3/2}}\frac{T_c^{3/2}}{Ze^2m_e^{1/2}\ln\Lambda}, \tag{13}$$

and

$$\mathbf{R}_h\equiv-\frac{e^2n_c}{\sigma}\int\mathbf{v}C(f_c^{(0)},f_h)\tau_{ei}(v)d^3\mathbf{v}. \tag{14}$$

This is just an expression of Ohm's law including the thermoelectric pressure ∇T_c term and the hot electron drag term, $\mathbf{R}_h$. The first is what is responsible for the voltage in a thermocouple wire. The second is the force per unit volume on the cold electrons due to collisions with the hot electrons. This can be more easily seen when the integral in Eq. (14) is evaluated to give

$$\mathbf{R}_h=-\left(\frac{m}{e\tau_{ch}}\right)\mathbf{J}_h, \tag{15}$$

where

$$\tau_{ch}\equiv\frac{3\sqrt{3}}{8\pi}\frac{m_e^{1/2}T_h^{3/2}}{n_ce^4\ln\Lambda}, \tag{16}$$

and $\mathbf{J}_h$ is the hot electron current. By quasineutrality, we can set $\mathbf{J}_h=-\mathbf{J}$. Assuming that $T_h\gg T_c$, one can neglect the hot electron drag term since it is smaller than $\mathbf{J}/\sigma$ by a factor $(T_c/T_h)^{3/2}$. This leaves us with the form of the cold electron momentum equation which we will use

$$\mathbf{E}=\frac{\mathbf{J}}{\sigma}-\frac{5}{2}\frac{1}{e}\nabla T_c. \tag{17}$$

The cold electron energy equation is found by taking the second-order velocity moment of Eq. (10). The result is

$$\frac{3}{2}n_c\frac{\partial T_c}{\partial t}=\mathbf{J}\cdot\mathbf{E}-\nabla\cdot\mathbf{q}-\frac{3}{2}\frac{T_c}{e}\nabla\cdot\mathbf{J}+Q_h, \tag{18}$$

where

$$\mathbf{q}=\int\frac{mv^2}{2}\mathbf{v}f_c^{(1)}\,d^3\mathbf{v} \tag{19}$$

and

$$Q_h=\int\frac{mv^2}{2}C(f_c^{(0)},f_h)d^3\mathbf{v}. \tag{20}$$

When the integral in Eq. (19) is evaluated using the form of $f_c^{(1)}$ found in Eq. (10) and the result substituted into Eq. (18), one is left with

$$\frac{3}{2}n_c\frac{\partial T_c}{\partial t}=\nabla\cdot(\kappa\nabla T_c)+\frac{J^2}{\sigma}-\frac{\mathbf{J}\cdot\mathbf{R}_h}{en_c}+Q_h+\frac{3}{2}\frac{1}{e}\mathbf{J}\cdot\nabla T_c+\frac{5}{2}\frac{T_c}{e}\nabla\cdot\mathbf{J}, \tag{21}$$

where

$$\kappa\equiv\frac{16\sqrt{2}}{\pi^{3/2}}\frac{T_c^{5/2}}{Ze^4m_e^{1/2}\ln\Lambda}. \tag{22}$$

The first term on the right-hand side of Eq. (21) is responsible for standard heat flow via thermal conduction. The second is the $J\cdot E$ heating term. As we already discussed $\mathbf{R}_h\ll en_c\mathbf{J}/\sigma$, so we neglect the third term. The drag of the hot electrons on the cold electrons transfers energy to the colds through the fourth term. This term can be written, when the integral for Q_h is evaluated, as

$$Q_h=\tfrac{3}{2}T_hn_h/\tau_{ch}. \tag{23}$$

The last two terms on the right-hand side of Eq. (21) are neglected because either $J=0$ or the sum of $J\cdot E$ and Q_h terms is larger than them. This can be seen most easily by assuming that the hot electron energy is deposited by the $J\cdot E$ and Q_h terms on a scale length L. The sum of the last two terms will be less than or of order J_0T_c/eL, where J_0 is the initial hot electron current. The two heating terms will be of order J_0T_h/eL, which is larger by a factor T_h/T_c. One can now write the cold electron energy equation as

$$\frac{3}{2}n_c\frac{\partial T_c}{\partial t}=\nabla\cdot(\kappa\nabla T)+\frac{J^2}{\sigma}+Q_h. \tag{24}$$

Now we turn our attention to the hot electron equation:

$$\frac{\partial f_h}{\partial t}+\mathbf{v}\cdot\frac{\partial f_h}{\partial\mathbf{x}}-\frac{e}{m_e}\mathbf{E}\cdot\frac{\partial f_h}{\partial\mathbf{v}}=C(f_h,f_i)+C(f_h,f_c), \tag{25}$$

where we have neglected the hot electron self-collision term since it will not contribute to the moment equations. To derive the momentum equation we take the first-order velocity moment of Eq. (25) and obtain

$$m_en_h\frac{d\mathbf{u}_h}{dt}+m_e\mathbf{u}_h\left(\frac{\partial n_h}{\partial t}+\nabla\cdot(n_h\mathbf{u}_h)\right)=-\nabla p-\nabla\cdot\mathbf{\Pi}-en_h\mathbf{E}+\int m_e\mathbf{v}C(f_h,f_i)d^3\mathbf{v}, \tag{26}$$

where

$$p\equiv m_en_h\langle(\mathbf{v}-\mathbf{u}_h)^2/3\rangle, \tag{27}$$

$$\mathbf{\Pi}\equiv m_en_h\left\langle\mathbf{vv}-\mathbf{I}\frac{(\mathbf{v}-\mathbf{u}_h)^2}{3}\right\rangle, \tag{28}$$

$$\int m_e\mathbf{v}C(f_h,f_i)d^3\mathbf{v}=-\frac{Z}{2}\frac{n_h\mathbf{u}_h}{\tau_{ch}}, \tag{29}$$

and we neglect the $C(f_h,f_c)$ term because $Z\gg1$.

The energy equation is found by taking the second-order velocity moment of Eq. (25). The result is

$$\frac{3}{2}T_h\left(\frac{\partial n_h}{\partial t}+\nabla\cdot(n_h\mathbf{u}_h)\right)$$

$$=-en_h\mathbf{E}\cdot\mathbf{u}_h+\int\frac{mv^2}{2}C(f_h,f_c)d^3\mathbf{v}, \tag{30}$$

where

$$\int\frac{mv^2}{2}C(f_h,f_c)d^3\mathbf{v}=-Q_h=-\frac{3}{2}\frac{T_hn_h}{\tau_{ch}}, \tag{31}$$

and the $C(f_h,f_i)$ term has been neglected since $Zm_e/m_i\ll 1$.

To neglect the hot electron inertia term on the left-hand side of Eq. (26), we assume that we are interested in evolution of the hot energy equation (or equivalently n_h) on a time scale τ_n that is much longer than that on which the velocity $\mathbf{u}_h$ evolves, τ_u; that is

$$\frac{1}{\tau_u}\sim\left|\frac{1}{\mathbf{u}_h}\frac{d\mathbf{u}_h}{dt}\right|\gg\left|\frac{1}{n_h}\left(\frac{\partial n_h}{\partial t}+\nabla\cdot(n_h\mathbf{u}_h)\right)\right|\sim\frac{1}{\tau_n}. \tag{32}$$

This will be true provided that $Z\gg 1$ and $|\mathbf{u}_h|\ll\sqrt{3T_h/m_e}$. The first condition will be true by assumption; the second we will have to enforce explicitly by a flux limiter. To see this ordering of time scales compare Eq. (26) to Eq. (30). First divide Eq. (26) by $m_en_h\mathbf{u}_h$ and Eq. (30) by T_hn_h. Note that the term involving $\mathbf{E}$ in Eq. (30) is smaller than the analogous term in Eq. (26) by the factor $|\mathbf{u}_h|/\sqrt{3T_h/m_e}$. One can also see that the term involving $C(f_h,f_c)$ in Eq. (30) is smaller than the term involving $C(f_h,f_i)$ in Eq. (26) by a factor $1/Z$.

We make a further assumption that the pressure is isotropic $\Pi=0$, and we are now left with the momentum equation

$$0=\nabla\cdot(n_hT_h)+en_h\mathbf{E}+\frac{Z}{2}\frac{n_h\mathbf{u}_h}{\tau_{ch}}. \tag{33}$$

For a 1-D problem Eqs. (17), (24), (30), and (33) can be reduced to

$$E=\frac{en_hu_h}{\sigma(T_c)}, \tag{34a}$$

$$\frac{3}{2}n_c\frac{\partial T_c}{\partial t}=\frac{\partial}{\partial x}\left(\kappa(T_c)\frac{\partial T_c}{\partial x}\right)+\frac{(en_hu_h)^2}{\sigma(T_c)}+\frac{3}{2}\frac{n_hT_h}{\tau_{ch}}, \tag{34b}$$

$$0=T_h\frac{\partial n_h}{\partial x}+en_hE+\frac{Z}{2}\frac{n_hm_eu_h}{\tau_{ch}}, \tag{34c}$$

$$\frac{\partial n_h}{\partial t}+\frac{\partial}{\partial x}(n_hu_h)=-\frac{(en_hu_h)E}{3T_h/2}-\frac{n_h}{\tau_{ch}}, \tag{34d}$$

where quasineutrality, $J=en_hu_h$, has been used and one must explicitly enforce $|u_h|\leqslant\sqrt{3T_h/m_e}$. Note that the ∇T_c term has been neglected in Eq. (34a). If it would have been retained and the resulting expression for E substituted into Eqs. (34c) and (34d), the additional term would be smaller than the others by a factor T_c/T_h. The logic that allows one to neglect this term is the same as that which allowed the ∇T_c terms to be neglected in Eq. (21). The injection of hot electrons into the problem will be done by the choice of the appropriate boundary conditions on Eqs. (34).

III. REGIMES OF TRANSPORT AND SCALING RELATIONSHIPS

The most convenient way to examine the regimes of transport and extract how different quantities scale with time, is to first cast the simple 1-D model developed in the previous section in dimensionless form. A natural velocity scale for the penetration of a current J_0 of suprathermal electrons into a cold dense background plasma of density n_c is the drift velocity, $u_0\equiv J_0/en_c$, required in the cold background plasma to neutralize the suprathermal current. One can now define a temperature, $T_0=m_eu_0^2$, and a frequency

$$1/\tau_0\equiv n_cu_0(e^2/T_0)^2Z\ln\Lambda. \tag{35}$$

For the remainder of this section, we normalize the densities by n_c, the temperatures by T_0, the times by τ_0, the distances by $u_0\tau_0$, and the velocities by u_0.

The first of the two coupled partial differential equations which constitute the simple 1-D model is Eq. (34b)

$$\frac{\partial T_c}{\partial t}=C\frac{\partial}{\partial x}\left(T_c^{5/2}\frac{\partial T_c}{\partial x}\right)+\left(\frac{2A}{3}\right)T_c^{-3/2}(n_hu_h)^2+\frac{2B}{Z}n_hT_h^{-1/2}, \tag{36a}$$

here written in dimensionless form. The second is Eq. (34d) with the substitution of the expression given for E in Eq. (34a)

$$\frac{\partial n_h}{\partial t}=-\frac{\partial}{\partial x}(n_hu_h)-\left(\frac{2A}{3}\right)\frac{T_c^{-3/2}}{T_h}(n_hu_h)^2-\frac{2B}{Z}n_hT_h^{-3/2}. \tag{36b}$$

By combining Eqs. (34a) and (34c) one obtains an expression for the hot electron fluid velocity,

$$n_hu_h^*=-T_h\frac{(\partial n_h/\partial x)}{(BT_h^{-3/2}+An_hT_c^{-3/2})}, \tag{37}$$

that must be flux limited so that the velocity used in Eqs. (36) is less than $\sqrt{3T_h}$. One can do this by setting

$$u_h=\min(u_h^*,\sqrt{3T_h}) \tag{38a}$$

or, in a more continuous way, by letting

$$u_h=\frac{u_h^*v_h}{u_h^*+v_h}, \tag{38b}$$

where $v_h\equiv\sqrt{3T_h}$. In these dimensionless equations, $A\equiv\pi^{3/2}/4\sqrt{2}$, $B\equiv 4\pi/3\sqrt{3}$, and $C\equiv 32\sqrt{2}/3\pi^{3/2}$ are constants.

The boundary conditions we use are that there is no heat flow at $x=0$ or $x=l$ and that there is no hot electron flow at $x=l$, where l is some large distance greater than the scale lengths of interest. The hot electron flow at $x=0$ that corresponds to a current of J_0 in our normalized units is $n_hu_h=1$. This leaves us with the following boundary conditions on Eqs. (36):

$$\frac{\partial T_c(x=0)}{\partial x}=\frac{\partial T_c(x=l)}{\partial x}=\frac{\partial n_h(x=l)}{\partial x}=0, \tag{39a}$$

and

$$n_h u_h(x=0)=1. \tag{39b}$$

The initial hot electron density and cold electron temperature are both assumed to be 0. This gives the initial conditions

$$n_h(t=0,x)=T_c(t=0,x)=0. \tag{40}$$

An easy identification of the collisional source of the terms on the right-hand side of Eqs. (36) and (37) can be made according to their constant coefficients. The $J\cdot E$ heating, as well as the cold resistivity, come from $C(f_c,f_i)$ and are those terms which involve A. The heat conductivity comes from the same collisional source and is the term with the C constant multiplier. The direct collisional energy exchange from the hot electrons to the cold electrons has its origin in $C(f_h,f_c)$. The corresponding drag heating terms are the two with the $2B/Z$ multipliers. Finally, the hot electron resistivity is caused by $C(f_h,f_i)$ and appears in Eq. (37) as the term with B.

The solutions of Eqs. (36) only depend on the parameters T_h and Z. In other words, one can write the solutions as $T_c(x,t;T_h,Z)$, $n_h(x,t;T_h,Z)$, and $u_h(x,t;T_h,Z)$. Given a value of T_h and Z all the solutions are just scaled versions of each other. For practical purposes it is necessary to know the quantities by which the variables are scaled in physical units. Assuming that there is an energy deposition into hot electrons of $I(\mathrm{W/cm^2})$ and that each hot electron has an energy $T_h(\mathrm{keV})$, one finds that

$$T_0(\mathrm{keV})=2\times10^{13}\,\frac{I^2(\mathrm{W/cm^2})}{n_c^2(/\mathrm{cc})T_h^2(\mathrm{keV})}, \tag{41a}$$

$$u_0(\mathrm{cm/s})=6\times10^{15}\,\frac{I(\mathrm{W/cm^2})}{n_c(/\mathrm{cc})T_h(\mathrm{keV})}, \tag{41b}$$

$$\tau_0(\mathrm{ps})=4.2\times10^{42}\,\frac{1}{Z\ln\Lambda}\,\frac{I^3(\mathrm{W/cm^2})}{n_c^4(/\mathrm{cc})T_h^3(\mathrm{keV})}, \tag{41c}$$

and

$$u_0\tau_0(\mathrm{cm})=2.7\times10^{50}\,\frac{1}{Z\ln\Lambda}\,\frac{I^4(\mathrm{W/cm^2})}{n_0^5(/\mathrm{cc})T_h^4(\mathrm{keV})}. \tag{41d}$$

A straightforward separation of the transport into temporal regimes or eras can now be done on the basis of what terms dominate; first, in the equation for T_c, Eq. (36a); and second, in the equation for n_h, Eq. (36b). Letting the scale length for the hot electron density be given by $L_n\sim n_h/(\partial n_h/\partial x)$ and the scale length for the cold electron temperature be given by $L_T\sim T_c/(\partial T_c/\partial x)$, one obtains the following relationships:

$$\frac{\partial T_c}{\partial t}\sim O\left(\frac{T_c^{7/2}}{L_T^2}\right)+O(T_c^{-3/2})+O\left(\frac{2B}{Z}\,n_hT_h^{-1/2}\right), \tag{42a}$$

$$\frac{\partial n_h}{\partial t}\sim O\left(\frac{1}{L_n}\right)-O\left(\frac{T_c^{-3/2}}{T_h}\right)-O\left(\frac{2B}{Z}\,n_hT_h^{-3/2}\right), \tag{42b}$$

and

$$L_n\sim\min\left(\frac{n_hT_h^{5/2}}{B},T_hT_c^{3/2},n_h(3T_h)^{1/2}L_n\right). \tag{42c}$$

The boundary condition has also been used in obtaining the above expressions, by involving the scaling $n_hu_h\sim O(1)$. It also has been assumed that $2A/3\sim C\sim O(1)$. The first two scaling relationships are consequences of Eqs. (36). The third is an expression of Eq. (37) using the flux limiter given in Eq. (38a). The terms on the right-hand side of Eq. (42c) correspond to hot electron resistivity, cold electron resistivity, and the flux limit, respectively.

Aiding in the separation of transport into regimes is the fact that $T_h\gg1$. This can be seen most easily from the statement of quasineutrality $n_hu_h=-n_cu_0$, which implies that $T_h\sim(n_c/n_h)^2\gg1$.

During the earliest times and smallest temperatures the $J\cdot E$ heating term dominates the temperature equation, the advective term dominates the density equation, and the flux is limited in the equation for L_n. Therefore, we find that

$$\frac{\partial T_c}{\partial t}\sim T_c^{-3/2}, \tag{43a}$$

$$\frac{\partial n_h}{\partial t}\sim\frac{1}{L_n}, \tag{43b}$$

$$L_n\sim n_h(3T_h)^{1/2}L_n, \tag{43c}$$

and that, because the cold electron heat flow is not significant, $L_T\sim L_n$. The solution to Eqs. (43) is $T_c\sim t^{2/5}$, $n_h\sim(3T_h)^{-1/2}$, and $L_n\sim L_T\sim(3T_h)^{1/2}t$. These scalings will hold as long as L_n is determined by its flux limited value, that is, $t\leqslant(3T_h)^{5/4}$. This temporal regime we call the *transient $J\cdot E$ regime*. Here, the hot electrons move unimpaired by the electric field setup to supply the cold return current. Meanwhile the cold background is heated by the $J\cdot E$ effect.

For later times the $J\cdot E$ heating term still dominates the temperature equation, the advective term still dominates the density equation, but the cold electron resistivity dominates the expression for L_n. This leaves us with

$$\frac{\partial T_c}{\partial t}\sim T_c^{-3/2}, \tag{44a}$$

$$\frac{\partial n_h}{\partial t}\sim\frac{1}{L_n}, \tag{44b}$$

$$L_n\sim T_hT_c^{3/2}, \tag{44c}$$

and $L_T\sim L_n$. The scalings which solve these equations are $T_c\sim t^{2/5}$, $n_h\sim T_h^{-1}t^{2/5}$, and $L_n\sim L_T\sim T_ht^{3/5}$. This is what we call the *$J\cdot E$ regime*, and it covers the time from when the transient $J\cdot E$ regime ends to the time when the $J\cdot E$ heating term in the temperature equation becomes of order the drag heating term, that is, $(3T_h)^{5/4}\leqslant t\leqslant T_h^{3/2}(Z/2B)$. During this regime, the hot electrons are being slowed down by the electric field. The reduction of the exponent of t in the expression for L_n is to allow some of the beam to sacrifice itself, heating the background, lowering the resistivity, and allowing the hot electrons to penetrate further.

As the background is heated, the importance of the $J\cdot E$ heating decreases. Eventually the next temporal regime is

TABLE I. Regimes of transport. The minimum time for which the regime's scalings are valid is $t_{\min}$.

	Transient $J\cdot E$	$J\cdot E$	Drag–$J\cdot E$ transition	Drag	Diffusion
$T_c\sim$	$t^{2/5}$	$t^{2/5}$	$t^{2/5}$	$T_h^{-1}\left(\frac{Z}{2B^2}\right)^{-1/2} t$	$T_h^{4/9}t^{2/9}$
$L_n\sim$	$(3T_h)^{1/2}t$	$T_h^{1}t^{3/5}$	$T_h^{1}t^{3/5}$	$T_h^{2}\left(\frac{Z}{2B^2}\right)^{1/2}$	$T_h^{2}\left(\frac{Z}{2B^2}\right)^{1/2}$
$L_T\sim$	$(3T_h)^{1/2}t$	$T_h^{1}t^{3/5}$	$T_h^{1}t^{3/5}$	$T_h^{2}\left(\frac{Z}{2B^2}\right)^{1/2}$	$T_h^{5/9}t^{7/9}$
$n_h\sim$	$(3T_h)^{-1/2}$	$T_h^{-1}t^{2/5}$	$\left(\frac{Z}{2B}\right)T_h^{1/2}t^{-3/5}$	$\left(\frac{Z}{2}\right)^{1/2}T_h^{-1/2}$	$\left(\frac{Z}{2}\right)^{1/2}T_h^{-1/2}$
$t_{\min}\sim$	0	$(T_h/3)^{5/4}$	$T_h^{3/2}\left(\frac{Z}{2B}\right)$	$T_h^{5/3}\left(\frac{Z}{2B^2}\right)^{5/6}$	$T_h^{13/7}\left(\frac{Z}{2B^2}\right)^{9/14}$

entered where the drag heating term dominates the temperature equation, the advective term in the density equation is balanced by the drag heating term, and the density scale length is still determined by the cold electron resistivity. One can now write

$$\frac{\partial T_c}{\partial t}\sim\frac{2B}{Z}n_hT_h^{-1/2}, \tag{45a}$$

$$\frac{1}{L_n}\sim\frac{2B}{Z}n_hT_h^{-3/2}, \tag{45b}$$

$$L_n\sim T_hT_c^{3/2}, \tag{45c}$$

and $L_n\sim L_T$. One can verify by simple substitution into the above equation that $T_c\sim t^{2/5}$, $n_h\sim(Z/2B)T_h^{1/2}t^{-3/5}$, and $L_n\sim L_T\sim T_ht^{3/5}$. This will be referred to as the *$J\cdot E$-drag transition regime*. It will span times from the end of the previous regime to those when the density scale length becomes dominated by hot electron collisionality, that is, $T_h^{3/2}(Z/2B)\leqslant t\leqslant T_h^{5/3}(Z/2B^2)^{5/6}$.

The *drag regime* is the next regime that is entered. The only change is the dominance of the hot electron collisionality in the equation for L_n, so that

$$\frac{\partial T_c}{\partial t}\sim\frac{2B}{Z}n_hT_h^{-1/2}, \tag{46a}$$

$$\frac{1}{L_n}\sim\frac{2B}{Z}n_hT_h^{-3/2}, \tag{46b}$$

$$L_n\sim\frac{1}{B}n_hT_h^{5/2}, \tag{46c}$$

and $L_n\sim L_T$. The solution of Eqs. (46) is $T_c\sim(2B^2/Z)^{1/2}T_h^{-1}t$, $n_h\sim T_h^{-1/2}(Z/2)^{1/2}$, and $L_n\sim L_T\sim T_h^2(Z/2B^2)^{1/2}$. One leaves this regime when the heat conduction term starts to dominate in the temperature equation so that the regime spans times such that $T_h^{5/3}(Z/2B^2)^{5/6}\leqslant t\leqslant T_h^{13/7}(Z/2B^2)^{9/14}$. Note that the width of the heated layer is a constant given by the geometric mean of the hot electron–ion mean free path, λ_{ei}, and the hot electron–cold electron mean free path, λ_{ee}. This is due to hot electrons randomly changing direction on a scale length determined by how fast they lose their momentum, λ_{ei}. The diffusion continues until they travel a long enough distance that they lose their energy, λ_{ee}.

The final regime comes into play when the temperature gradient becomes so large that thermal diffusion can carry the deposited energy deeper into the background plasma. The heat conduction term dominates in this, the *diffusive regime*, so that one can write

$$\frac{\partial T_c}{\partial t}\sim\frac{T_c^{7/2}}{L_T^2}, \tag{47a}$$

$$\frac{1}{L_n}\sim\frac{2B}{Z}n_hT_h^{-3/2}, \tag{47b}$$

and

$$L_n\sim\frac{1}{B}n_hT_h^{5/2}. \tag{47c}$$

The boundary condition specifies that the heat flow must be equal to the incident energy flux, $T_c^{7/2}/L_T\sim O(T_h)$. The well-known similarity solution[28] exists for T_c, such that $T_c\sim T_h^{4/9}t^{2/9}$, $n_h\sim T_h^{-1/2}(Z/2)^{1/2}$, $L_n\sim T_h^2(Z/2B^2)^{1/2}$, and $L_T\sim T_h^{5/9}t^{7/9}$.

An overview of the regimes is given in Table I. The relationship of these transport regimes to each other can be seen in Fig. 1. Here for a fixed value of $Z=79$, gold, the areas in (t,T_h) space where the different processes dominate are shown. Note that there is a well-ordered temporal progression through the regimes for a fixed value of T_h. A sample of how the quantities scale with time for a value of $T_h=10^4$ is shown in Fig. 2. Compared to these simple scalings is a numerical solution of Eqs. (36) with the continuous flux limiter given in Eq. (38b). These equations, which reduce to two coupled 1-D nonlinear parabolic partial differential equations, were solved using a predictor–corrector algorithm.[29] There is good agreement in the scaling behavior, but a factor of 4 discrepancy exists in the L_n values for the $J\cdot E$ regime. The density of hot electrons at the surface, n_h, and hence the hot electron pressure peaks at the end of the $J\cdot E$ regime. Its maximum value is

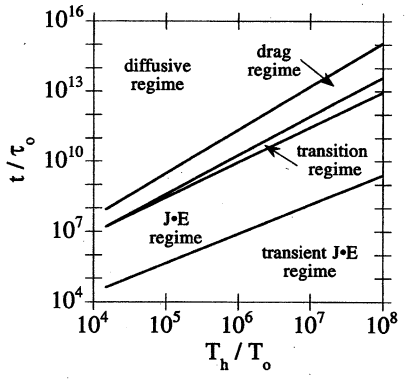

FIG. 1. Areas in (t,T_h) space where the different transport processes dominate. The location of the transport regimes are shown for $Z=79$.

$$(n_h)_{\max}=\left(\frac{Z}{2}\right)^{1/2} T_h^{-1/2}\left(\frac{T_h}{B^4 Z/2}\right)^{1/10}.$$

This is enhanced above the time asymptotic diffusive value of $(Z/2)^{1/2}T_h^{-1/2}$ by the inhibition of the transport by the electric fields. This electric field is also evidenced by range shortening of L_n to a value below its free-streaming value of $\min[(3T_h)^{1/2}t,(Z/2B^2)^{1/2}T_h^2]$.

IV. COMPARISON OF THE SIMPLE MODEL TO LASNEX

A severe assumption of the simple model is that there is only one group of hot electrons. There is no *a priori* reason why only one group should be sufficient to capture the character of the transport. For this reason, a comparison was made between the multigroup diffusion method[17] of hot electron transport used in LASNEX[19] and the numerical solution of Eqs. (36). We used a Maxwellian source of hot electrons in LASNEX with energy $T_h=100$ keV and energy flux 3×10^{17} W/cm^2, that was injected into the first cell of a 1-D LASNEX calculation. These electrons were allowed to transport into a hydrogen plasma of constant density 0.24 g/cc. Hydrodynamic motion of the plasma, radiation generation, and radiation transport were disabled. Twenty groups were used in the hot electron transport. The results are shown in Fig. 3. They are compared to the numerical solution of the simple model with $Z=1$ and $T_h/T_0=10^4$. As one can see, the two models show good agreement over many decades in time that span all five transport regimes. The discrepancy in the temperature at early times is due to the condensed matter[30] low temperature conductivity used in LASNEX.

V. IMPLICATIONS AND APPLICATIONS OF THE SIMPLE MODEL

A. Fast ion generation

A use of the simple model is to determine the amount of energy that will be transferred into fast ions at the front surface of a plasma, if the laser ponderomotive force is neglected. There has been much experimental, theoretical, and modeling work[31] done on the transfer of hot electron energy into the hydrodynamic energy of energetic ions blown off of the surface of the plasma. This blowoff is caused by the hot electrons which strike the surface of the plasma and try to

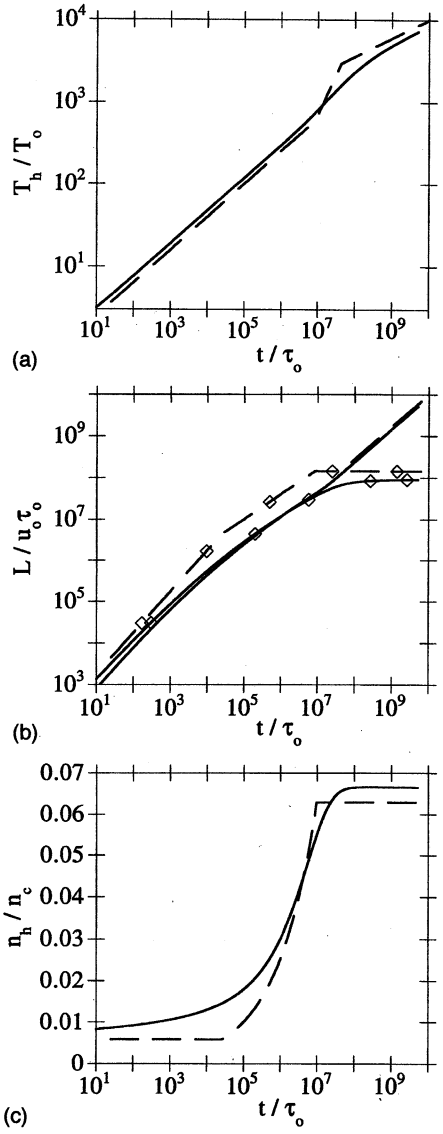

FIG. 2. Time dependence of physical quantities for $Z=79$ and $T_h=10^4$. Solid lines are the numerical solution of Eqs. (36). Dashed lines are the simple scalings given in Table I. (a) Temperature at the surface ($x=0$) where laser energy is deposited into suprathermal electrons. (b) Depth to which electrons penetrate L_n shown as lines with diamonds. Depth to which heat is transported by thermal diffusion L_T is shown by the plain lines. Values for numerical solution are the depths for which n_h and T_c reach one-half their surface values. (c) Density of suprathermal electrons at the surface.

leave. Because the Debye length for the hot electrons is small compared to the distance that the ions will move during their acceleration phase, there is no significant charge separation and the hot electrons will bounce off the wall formed by the edge of the ion density. As the hot electrons bounce off the wall they will transfer momentum to the ions. Since the simple model gives the density of the hot electrons at the surface, one can estimate the rate at which energy is being transferred from the hot electrons to the ions. One should note that the simple model is only being used to estimate the density of hot electrons which enter this blowoff region at the edge of the plasma. Within this blowoff region there will be only hot electrons and assumptions of the simple model such as $n_h \ll n_c$ will be violated, but there is

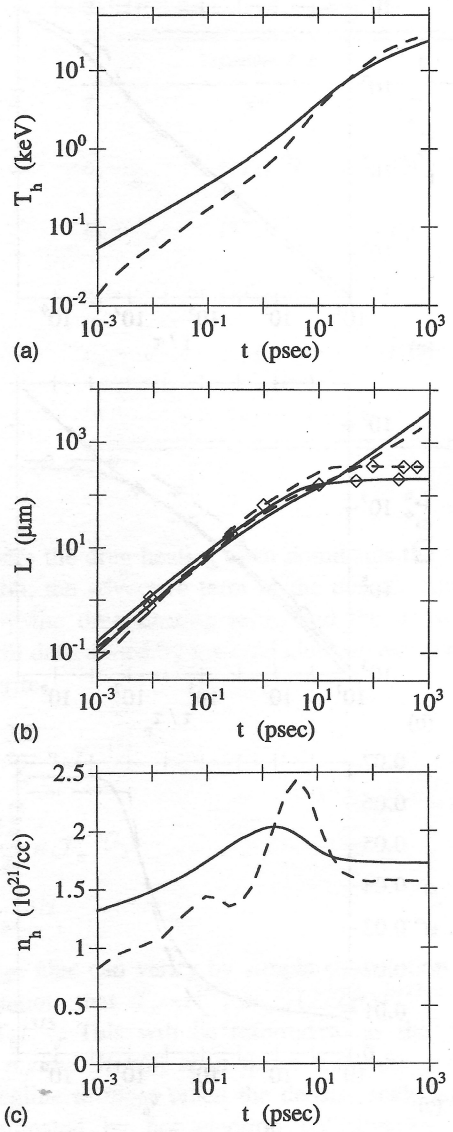

FIG. 3. Comparison of 1-D LASNEX multigroup electron diffusion solution (dashed lines) to numerical solution of Eqs. (36) (solid lines). An energy flux of 3×10^{17} W/cm^2 is put into 100 keV electrons which transport into a hydrogen plasma of density of 0.24 g/cc. (a) Temperature at $x=0$. (b) Depths at which n_h (lines with diamonds) and T_c reach one-half their value at $x=0$. (c) Density of suprathermal electrons at $x=0$.

also no transfer of energy from the hot electrons to the cold electrons in this region. Since we will find that hot electrons lose most of their energy to the cold electrons, the density of the hot electrons is being determined by the transport in the bulk of the plasma where the simple model can be applied.

We now turn our attention to a quantitative estimate of the energy exchange using the simple model. The rate at which momentum is being transferred from the hot electrons to the ions is the flux of hot electrons on the surface times their momentum

$$\frac{1}{\text{area}}\frac{dp_i}{dt}=(n_h v_h)(m_e v_h). \tag{48}$$

The energy exchange rate will be

TABLE II. Amount of suprathermal electron energy coupled into ion hydromotion (fast ions).

	Simple model	LASNEX
Hydrogen	4%	4%
Solid gold	12%	11%
Hydrogen on solid gold	18%	18%

$$\frac{1}{\text{area}}\frac{dE_i}{dt}=v_i\frac{1}{\text{area}}\frac{dp_i}{dt}\sim n_h T_h v_i. \tag{49}$$

What remains to be found is an expression for the ion expansion velocity. This can be done most easily by equating the energy contained in the ion blowoff layer of thickness d to the time integral of the energy exchange rate

$$\frac{n_h}{Z}(m_i v_i^2)d\sim\int_0^t\frac{1}{\text{area}}\frac{dE_i}{dt}\,dt\sim n_h T_h d. \tag{50}$$

Therefore, the ion expansion velocity will be the ion sound speed using the hot electron temperature

$$v_i\sim\left(\frac{Zm_e}{m_i}\right)^{1/2}\left(\frac{T_h}{m_e}\right)^{1/2}. \tag{51}$$

When this is compared to the rate at which energy is being deposited into the hot electrons dE_h/dt, one finds that

$$\frac{dE_i/dt}{dE_h/dt}\sim\left(\frac{n_h}{n_c}\right)\left(\frac{T_h}{T_0}\right)^{1/2}\left(\frac{Zm_e}{m_i}\right)^{1/2}. \tag{52}$$

The expression for n_h/n_c from Table I can be substituted into Eq. (52) to find the time dependence of the energy being put into the ion blowoff. This energy transfer rate is maximized at the end of the $J\cdot E$ regime when

$$\left(\frac{dE_i/dt}{dE_h/dt}\right)_{\max}\sim\left(\frac{Z}{2}\right)^{1/2}\left(\frac{Zm_e}{m_i}\right)^{1/2}\left[\left(\frac{T_h}{T_0}\right)\frac{1}{B^4Z/2}\right]^{1/10}. \tag{53}$$

The second factor is, for most cases, approximately equal to 1/40. The first factor is just how many "effective" times the hot electron hits the surface before it loses its energy to the cold electrons, neglecting electric fields. Each time it hits the surface it loses 1/40 of its energy. This can be enhanced mildly by electric fields as determined by the third factor.

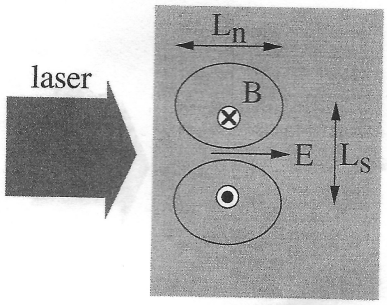

FIG. 4. Geometry of azimuthal magnetic field. Laser energy deposited into hot electrons. Electric field formed to drive return current in cold background plasma to cancel hot electron current. Curl of this electric field generates the magnetic field.

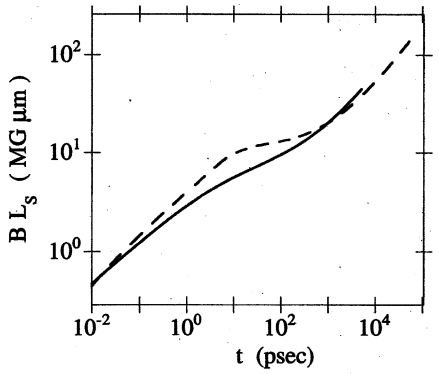

FIG. 5. Azimuthal magnetic field amplitude versus time. The laser spot diameter is given by L_s. Solid lines are the numerical solution of Eqs. (36). Dashed lines are the simple scalings given in Table I. An energy flux of 3×10^{17} W/cm^2 is put into 100 keV electrons which transport into a hydrogen plasma of density of 0.24 g/cc.

The energy put into the ions is therefore significantly enhanced in high Z, high density plasmas ($n_c \gg n_h$ which implies $T_h \gg T_0$).

We have compared the LASNEX estimate of fast ion blowoff to that of the simple model. For this comparison we modeled the 1-D transport of a suprathermal electron pulse (1 ps, 10^{17} W/cm^2, 80 keV) into hydrogen (density of 1 g/cc), solid gold, and 500 Å of hydrogen on top of solid gold. The amount of the suprathermal electron energy transferred into

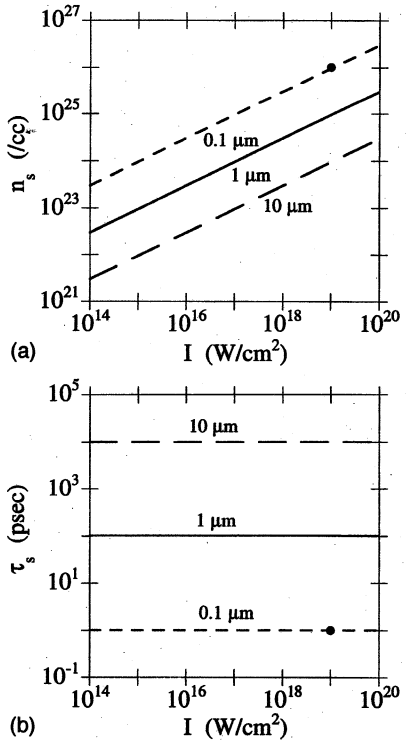

FIG. 6. Similar plasma conditions. Conditions that have equivalent transport to the absorption of an intense laser ($I=10^{19}$ W/cm^2, $\lambda=0.1$ μm, $\tau_{pulse}=1$ ps) into a dense precompressed core $n_c=10^{26}$/cc are shown. Small dashed lines are the conditions for a 0.1 μm laser. Large dashed lines are the conditions for a 10 μm laser. Solid lines are the conditions for a 1 μm laser. Large dots are the above unscaled conditions.

TABLE III. Example electron transport conditions.

Condition	I (W/cm^2)	t_{pulse} (ps)	n_c (/cc)	T_h (keV)
A	10^{16}	750	10^{22}	200
B	10^{18}	1	10^{23}	200
C	10^{19}	0.1	10^{23}	1000
D	10^{19}	1	10^{26}	100
E	10^{15}	100	10^{24}	10
F	10^{16}	750	10^{24}	200

ion hydromotion was calculated. These LASNEX simulations included local thermodynamic equilibrium (LTE) atomic physics, hydrodynamics, and multigroup electron transport. In Table II, the results of the computer simulations are compared to the prediction of the simple model given above. For the case of the hydrogen on solid gold a $Z/A=1$ was used in the second factor of Eq. (52) instead of 79/197, the appropriate value for solid gold. This was done because the hydrogen ions are being accelerated instead of the gold ions while the hot electron density is still being determined by the transport in the bulk gold. The electron density used in the simple model for solid gold was the same as that calculated in the simulations and was consistent with an ionization state of $Z^*=25$. An interesting trend should be noted in these data. Pure hydrogen couples less than 1/4 the energy into fast ions that solid gold with some surface hydrogen does.

B. Magnetic field generation

Another application of the simple model is to estimate the time dependence of the magnetic fields that will be generated by the electric field, $E=J/\sigma$. These are fields that are formed behind the laser spot. Their geometry is shown in Fig. 4. We assume that the problem is still approximately 1-D or that the length scales of interest are less than the laser spot size, L_s. From Maxwell's equations $\dot{B}\approx -c\nabla\times E$. Therefore, one finds that $\dot{B}\sim cE/L_s$ since E is directed perpendicular to the laser absorption surface and it diminishes in the direction parallel to the surface. The electric field can be rewritten from Eq. (34a) as

$$E=B_0(AZ\ln\Lambda)(T_c/T_0)^{-3/2}, \tag{54}$$

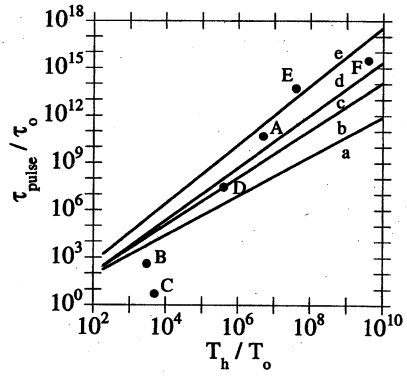

FIG. 7. Electron transport conditions given in Table III shown in (t,T_h) space. Areas where different transport regimes occur for $Z=1$ are also displayed: (a) transient $J\cdot E$ regime, (b) $J\cdot E$ regime, (c) $J\cdot E$-drag transition regime, (d) drag regime, and (e) diffusion regime.

where $B_0 \equiv e^3 n_c / T_0$. In physical units,

$$B_0(\mathrm{G}) = 3.2\times10^{-33}\,\frac{n_c^3(/\mathrm{cc})\,T_h^2(\mathrm{keV})}{I^2(\mathrm{W/cm^2})}. \tag{55}$$

Using the cold electron temperature scalings found in Table I, one finds that B scales as $t^{2/5}$ during the first three regimes, does not increase during the drag regime, and increases again as $t^{2/3}$ during the diffusive regime. For example, we plot in Fig. 5 the magnetic field amplitude for the same parameters that were used to generate the data in Fig. 3. Shown is both the prediction using the T_c given by the scaling relationships in Table I, and the T_c obtained by numerical solution of Eqs. (36).

C. Similar plasma conditions

One can also use the similarity of the solutions for the same value of T_h/T_0 and Z, to determine scaled versions of the same electron transport conditions. For instance, take the transport of hot electrons ($T_h \approx 100$ keV) generated by an intense laser beam ($I=10^{19}$ W/cm^2, $\lambda=0.1$ μm, $\tau_{\mathrm{pulse}}=1$ ps) into a dense precompressed core $n_c=10^{26}$/cc. This cannot yet be done but one might like to see if there is a scaled version of this transport that one can do with existing lasers. Assuming that the hot electron temperature characteristic of resonance absorption is proportional to $T_h \propto (I\lambda^2)^{1/3}$,[1] one needs to find other situations that have the same value of T_h/T_0 and t/τ_0. Given the laser intensity I_s and wavelength λ_s one would like to use, the cold electron density n_s and the pulse length τ_s that would give similar transport are

$$n_s = n_c\left(\frac{I_s}{I}\right)^{1/2}\left(\frac{\lambda_s}{\lambda}\right)^{-1} \tag{56}$$

and

$$\tau_s = \tau_{\mathrm{pulse}}\left(\frac{\lambda_s}{\lambda}\right)^{2}. \tag{57}$$

These conditions are displayed graphically in Fig. 6. The unscaled conditions are shown as large dots on these graphs. Note that a 10^{15} W/cm^2, 1 μm laser with a pulse length of 100 ps, shot into a solid density target gives the same transport.

It is also instructive to place various lasers and plasma conditions on a $(T_h/T_0, t/\tau_0)$ plot. The common laser plasma conditions given in Table III, have been put on such a plot in Fig. 7. One can easily see the roughly equivalent conditions and those which lie in vastly different regimes.

D. Predicting *E*-field transport inhibition

As was discussed at the end of Sec. III, there can be significant inhibition of the hot electron transport by the electric field set up to supply the cold return current necessary to maintain quasineutrality. This happens during both the $J\cdot E$ and $J\cdot E$-drag transition regimes. The maximum inhibition occurs at the border between these two regimes. Some experiments have measured such inhibition.[32] The transport of 14 keV hot electrons generated by the absorption of a 1 μm, 3×10^{15} W/cm^2 laser was studied by monitoring the $K\alpha$ x-ray emission form the back side of a foil target. Gold targets of solid density and 0.5% solid density were used. For this experiment, only the density of the target foil n_c was varied. The hot electron temperature T_h, the hot electron current J_0, and the laser pulse length, $\tau=1$ ps, were held fixed. Assuming an average ionization state, $Z^*=30$, characteristic of a solid density Au plasma at a temperature of a few hundred volts[28] we have plotted the region of inhibited electron transport in Fig. 8. The location, for this experiment, of the two gold foils of different densities are shown relative to this region. As was measured in the experiment, the solid gold foil is three decades past the time when the transport would be inhibited. In contrast, the 0.5% solid density gold foil sits on the border of the transport inhibition region, where one can expect the range to be shortened by a factor of 2 to 4 from the formula given at the end of Sec. III. This was confirmed by the experiment.

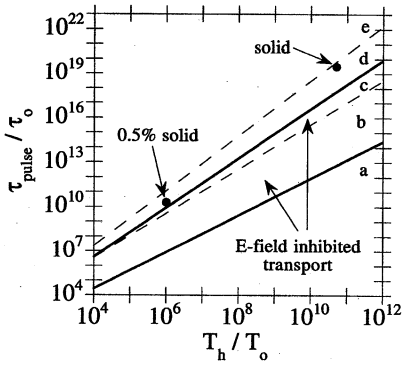

FIG. 8. Region of inhibition of transport by E field. Region of inhibition (for $Z^*=30$) is located between two solid lines. Shown as the large points are the transport conditions for 14 keV electrons into solid density gold and 0.5% solid density gold. A 2% absorption of a 3×10^{15} W/cm^2, 100 ps laser pulse is assumed. The regions of transport are also shown: (a) transient $J\cdot E$ regime, (b) $J\cdot E$ regime, (c) $J\cdot E$-drag transition regime, (d) drag regime, and (e) diffusion regime.

VI. CONCLUSIONS

The simple model and scaling relationships for suprathermal electron transport developed in this paper provide a framework against which more complicated models may be examined. By locating in which regime the transport lies, the dominant collisional effects and the general behavior of the complicated solutions can be predicted. Conversely, the results of parameter studies with the more complicated models can be organized according to the value of T_h/T_0 and t/τ_0 (as done in Fig. 7).

Estimates can be made with the simple model of physical effects which occur in laser heated plasmas, such as fast ion and magnetic field generation, that are consequences of the transport. The scaling relationships, found in Table I, can be easily applied to make basic arguments like those found in Sec. V. The product is a straightforward understanding of the cause of the effect.

Finally, one can identify, with the help of this model, physical situations that are superficially quite different in their character but demonstrate equivalent suprathermal electron transport.

ACKNOWLEDGMENTS

The author would like to thank Max Tabak, Bill Kruer, Jim Hammer, and Jim Albritten for useful discussion during the course of this research.

This work was supported by a U.S. Department of Energy Distinguished Postdoctoral Fellowship, and was performed under the auspices of the U.S. Department of Energy by the Lawrence Livermore National Laboratory under Contract No. W-7405-ENG-48.

[1]K. G. Estabrook and W. L. Kruer, Phys. Rev. Lett. **40**, 42 (1978).
[2]S. Wilks, W. L. Kruer, M. Tabak, and A. B. Langdon, Phys. Rev. Lett. **69**, 1383 (1992).
[3]W. L. Kruer and K. G. Estabrook, Phys. Fluids **28**, 430 (1985).
[4]K. G. Estabrook, W. L. Kruer, and B. F. Lasinski, Phys. Rev. Lett. **45**, 1399 (1980); K. G. Estabrook and W. L. Kruer, Phys Fluids **26**, 1892 (1983).
[5]F. Brunel, Phys. Rev. Lett. **59**, 52 (1987).
[6]R. J. Mason, Phys. Rev. Lett. **42**, 239 (1978).
[7]I. B. Bernstein, Phys. Fluids **20**, 577 (1977).
[8]T. Hsu, J. L. Hirshfield, and I. B. Bernstein, Phys. Fluids **21**, 413 (1978).
[9]D. Mosher, Phys. Fluids **18**, 846 (1975).
[10]H. A. Bethe, M. E. Rose, and L. P. Smith, Proc. Am. Philos. Soc. **78**, 573 (1938).
[11]J. R. Albritton, Phys. Rev. Lett. **50**, 2078 (1983).
[12]J. P. Matte and J. Virmont, Phys. Rev. Lett. **49**, 1936 (1982).
[13]A. R. Bell, R. G. Evans, and D. J. Nicholas, Phys. Rev. Lett. **46**, 243 (1981).
[14]T. Yabe, K. Mima, K. Yoshikawa, H. Takabe, and M. Hamano, Nucl. Fusion **21**, 803 (1981).
[15]M. Tabak, J. Hammer, M. E. Glinsky, W. L. Kruer, S. C. Wilks, J. Woodworth, E. M. Campbell, M. D. Perry, and R. J. Mason, Phys. Plasmas **1**, 1626 (1994).
[16]See National Technical Information Service Document No. UCRL-51121-73-2 (J. H. Nuckolls, "Laser fusion," in Laser-Fusion Program Semiannual Report, July–December 1973). Copies may be ordered from the National Technical Information Service, U.S. Department of Commerce, 5285 Port Royal Road, Springfield, Virginia 22161.
[17]See National Technical Information Service Document No. DE-83002429 (D. S. Kershaw, "Computer simulation of suprathermal transport for laser fusion," in Laser Program Annual Report 80, UCRL-50021-80). Copies may be ordered from the National Technical Information Service, U.S. Department of Commerce, 5285 Port Royal Road, Springfield, Virginia 22161.
[18]D. P. Murphy, M. Raleigh, R. E. Penchacek, and J. R. Greig, Phys. Fluids **30**, 232 (1987).
[19]G. B. Zimmerman and W. L. Kruer, Comments Plasma Phys. Controlled Fusion **2**, 85 (1975).
[20]L. E. Thode, Phys. Fluids **19**, 305 (1976).
[21]See National Technical Information Service Document No. AD-757790 (T. M. O'Neil and M. N. Rosenbluth, "Two-stream coupling of corona and core in laser-heated pellets," in Institute for Defense Analysis Report HQ 72-14450, 1972). Copies may be ordered from the National Technical Information Service, U.S. Department of Commerce, 5285 Port Royal Road, Springfield, Virginia 22161.
[22]W. L. Kruer, *The Physics of Laser Plasma Interactions* (Addison–Wesley, Redwood City, CA, 1988), p. 148.
[23]A. Rubenchik and S. Witkowski, *Handbook of Plasma Physics: Physics of Laser Plasmas, Volume III* (North-Holland, Amsterdam, 1991), pp. 519–547.
[24]J. A. Stamper, Laser Part. Beams **9**, 841 (1991).
[25]M. N. Rosenbluth, W. M. McDonald, and D. L. Judd, Phys. Rev. **107**, 1 (1957).
[26]E. M. Lifshitz and L. P. Pitaevskii, *Physical Kinetics* (Pergamon, Oxford, 1981), pp. 168–216.
[27]S. I. Braginskii, Rev. Plasma Phys. **1**, 205 (1965).
[28]Y. B. Zeldovich and Y. P. Raizer, *Physics of Shock Waves and High-Temperature Hydrodynamic Phenomena* (Academic, New York, 1966), pp. 664–668, 201–207.
[29]W. F. Ames, *Numerical Methods for Partial Differential Equations* (Academic, New York, 1977), pp. 85–89.
[30]Y. T. Lee and R. M. More, Phys. Fluids **27**, 1273 (1984).
[31]S. J. Gitomer, R. D. Jones, F. Begay, A. W. Ehler, J. F. Kephart, and R. Kristal, Phys. Fluids **29**, 2679 (1986).
[32]D. J. Bond, J. D. Hares, and J. D. Kilkenny, Phys. Rev. Lett. **45**, 252 (1980).